DETC2016-60064

A REGULARIZED CONTACT MODEL FOR MULTIBODY SYSTEM SIMULATION

Albert Peiret
Department of Mechanical Engineering
and Centre for Intelligent Machines
McGill University, Montréal, Canada
Email: alpeiret@cim.mcgill.ca

Farnood Gholami
Department of Mechanical Engineering
and Centre for Intelligent Machines
McGill University, Montréal, Canada
Email: farnood.gholami@mail.mcgill.ca

József Kövecses
Department of Mechanical Engineering
and Centre for Intelligent Machines
McGill University, Montréal, Canada
Email: jozsef.kovecses@mcgill.ca

Josep M. Font-Llagunes
Department of Mechanical Engineering and
Biomedical Engineering Research Centre
UPC, Barcelona, Spain
Email: josep.m.font@upc.edu

ABSTRACT

Simulation of large-scale multibody systems with unilateral contacts requires formulations with which good computational performance can be achieved. The availability of many solver algorithms for Linear Complementarity Problems (LCP) makes the LCP-based formulations a good candidate for this. However, considering friction in contacts asks for new friction models compatible with this kind of formulations. Here, a new, regularized friction model is presented to approximate the Coulomb model, which allows to formulate the multibody system dynamics as a LCP with bounds. Moreover, a bristle approach is used to approximate the stiction force, so that it improves the numerical behaviour of the system and makes it able to handle redundancy coming from the friction interfaces. Several examples using a 3D wheel model has been carried out, and the proposed friction model shows a better approximation of the Coulomb model compared to other LCP-based formulations.

INTRODUCTION

The simulation of multibody systems with contacts presents some well-known challenges, especially when it involves frictional contacts. Moreover, dealing with large systems and many contacts makes it more difficult to achieve good simulation performance. Several formulations have been proposed in the form of Linear Complementarity Problems (LCP), for which several direct or iterative solution algorithms are available.

LCP formulations expressed in the acceleration level were proposed in the literature [1, 2], but they are not guaranteed to always have a solution. This was the motivation to propose LCP formulations at the velocity-level, initially proposed by Anitescu and Potra [3] where *time-stepping* methods are incorporated in the dynamic formulation [4]. Such a formulation was proven to always have a solution [3], and hence, thus far it has been widely used for contact dynamics of multibody systems [5–7].

Generally, in velocity-level formulations penetration between the interacting bodies can happen. As an alternative formulation, the LCP can be expressed at the position-level [8]. Such a formulation can guarantee that no penetration occurs by the position-level constraint imposition, though allowable motion of the interacting bodies can be unrealistically restricted [9].

All these formulations rely on the polygonal approximation of the Coulomb friction cone, so that the resulting formulation is a mixed LCP. On the other hand, Lacoursiere [10] proposed the box approximation which allows to formulate a LCP with bounds; the most general formulation for a LCP.

To solve a LCP, a well-known category of approaches is based on the *symplex methods*, which are known as the *direct* or *pivoting methods* as well. Various pivoting algorithms are available for this purpose, such as the one proposed by Júdice and Pires [11]. Direct methods are usually used when accurate and robust simulations are required and enough computational time is available.

Additionally, with the aim of improving the static behaviour of the Coulomb model, several authors [12–15] have proposed friction models using the *bristle approach*. Essentially, the surface asperities are modelled with flexible bristles, so that a constitutive relationship is used to approximate the static friction force.

Some of these so-called dynamic models [12, 15] are very detailed, and its implementation in large-scale multibody system has not yet been done successfully. However, a simpler model was proposed by Liang et al. [13], an extension to contact in 3-dimensional space of the model by Haessig and Friedland [14]. There, a linear viscous-elastic element is used to define the stiction force.

In this work, a new regularized friction model is presented to approximate the Coulomb model. The static force is regularized using a bristle model, while the kinetic force is regularized with a hybrid approach between dry and viscous friction. This allows for formulating the dynamics model of a multibody system as a mixed LCP with bounds. The dynamic equations are formulated at the velocity-level, so that the velocities are the main variables together with the constraint and friction forces.

MULTIBODY SYSTEM DYNAMICS

Let $\mathbf{q}$ be the $p \times 1$ array of generalized coordinates of a multibody system. A set of n generalized velocities $\mathbf{v}$ is defined, such that $\dot{\mathbf{q}} = \mathbf{\Gamma v}$, where $\mathbf{\Gamma}(\mathbf{q}, t)$ is the $p \times n$ transformation matrix. With this representation of the system, the dynamic equations are

$$\mathbf{M}\dot{\mathbf{v}} + \mathbf{c} = \mathbf{f}_{app} + \mathbf{f}_{bilat} + \mathbf{f}_{cont} + \mathbf{f}_{fric} \qquad (1)$$

where $\mathbf{M}(\mathbf{q})$ is the $n \times n$ mass matrix, $\mathbf{c}(\mathbf{q}, \mathbf{v})$ is the $n \times 1$ array containing the Coriolis and centrifugal terms, $\mathbf{f}_{app}$ is the generalized applied force, $\mathbf{f}_{bilat}$ and $\mathbf{f}_{cont}$ are the generalized bilateral and unilateral constraint forces, respectively, and $\mathbf{f}_{fric}$ is the generalized friction force.

The m bilateral constraints (holonomic and linear nonholonomic) are defined at the velocity level as

$$\mathbf{u} = \mathbf{A v} \qquad (2)$$

where $\mathbf{A}(\mathbf{q})$ is the $m \times n$ constraint Jacobian matrix, and $\mathbf{u}(\mathbf{q}, t)$ is a $m \times 1$ array of given functions, which usually are equal to zero.

Then, the generalized bilateral constraint force is $\mathbf{f}_{bilat} = \mathbf{A}^T \boldsymbol{\lambda}$, where $\boldsymbol{\lambda}$ is the $m \times 1$ array of Lagrange multipliers.

For the r contacts, i.e., unilateral constraints, the *gap functions* that define the distance between contacting surfaces are arranged into the array $\boldsymbol{\Phi}(\mathbf{q}) \geq \mathbf{0}$, so the normal separation velocity can be expressed as

$$\dot{\boldsymbol{\Phi}} = \mathbf{N v} \qquad (3)$$

where $\mathbf{N}(\mathbf{q})$ is the $r \times n$ contact Jacobian matrix. The generalized contact force is $\mathbf{f}_{cont} = \mathbf{N}^T \boldsymbol{\lambda}_N$, where $\boldsymbol{\lambda}_N$ contains the r normal forces, which will be defined below.

The tangent plane of each contact point is characterized using two orthogonal directions, in which the components of the sliding velocity at the contact points can be expressed as

$$\mathbf{v}_T = \mathbf{D v} \qquad (4)$$

where $\mathbf{D}(\mathbf{q})$ is the $2r \times n$ friction Jacobian matrix. Then, the generalized friction force is $\mathbf{f}_{fric} = \mathbf{D}^T \boldsymbol{\lambda}_T$, where $\boldsymbol{\lambda}_T$ is the array that contains the $2r$ components of the friction forces, which will be defined below.

Discrete-Time Representation

The velocity-level formulation is achieved by means of a finite difference approximation of the acceleration as following

$$\dot{\mathbf{v}}^+ = \frac{\mathbf{v}(t+h) - \mathbf{v}(t)}{h} = \frac{\mathbf{v}^+ - \mathbf{v}}{h} \qquad (5)$$

where the superscript $^+$ is used for the unknown variables in the time-step, so that $\mathbf{v}^+$ and $\dot{\mathbf{v}}^+$ contain the unknown generalized velocities and accelerations respectively, and h is the time-step size.

The generalized accelerations are found in the dynamic equations

$$\mathbf{M}\dot{\mathbf{v}}^+ + \mathbf{c} = \mathbf{f}_{app} + \mathbf{f}_{bilat}^+ + \mathbf{f}_{cont}^+ + \mathbf{f}_{fric}^+ \qquad (6)$$

where the generalized forces $\mathbf{f}^+$ are defined *implicitly* using the unknown velocities $\mathbf{v}^+$; while the other unspecified elements, such as the mass matrix $\mathbf{M}$, and $\mathbf{c}$ and $\mathbf{f}_{app}$ vectors, are computed *explicitly* using the known mechanical state $\mathbf{q}$ and $\mathbf{v}$. This notation for the known and unknown variables is kept along the paper.

On the other hand, the generalized coordinates are updated *explicitly* using the known $\mathbf{q}$ and $\mathbf{v}$ as following

$$\mathbf{q}^+ = \mathbf{q} + h\mathbf{\Gamma v} \qquad (7)$$

Copyright © 2016 by ASME

This integration together with the Eqn. (5) give to this formulation a *semi-implicit* approach, so that the energy drift – due to the numerical integration – is reduced, compared to a fully implicit formulation.

FRICTION MODEL

The Coulomb model has proven to be very representative for the friction in contacts. However, its use in large system simulation makes it hard to achieve good simulation performance. To overcome this, a regularized friction model is proposed to approximate the Coulomb model, which distinguishes between static and kinetic phases.

In this section, the formulation is derived for one contact point in order to lighten the notation. Therefore, the sliding velocity and the friction force are

$$\mathbf{v}_T = \mathbf{D}\mathbf{v} = \begin{bmatrix} v_{T1} \\ v_{T2} \end{bmatrix} \quad \text{and} \quad \boldsymbol{\lambda}_T = \begin{bmatrix} \lambda_{T1} \\ \lambda_{T2} \end{bmatrix} \tag{8}$$

Static Friction Model

The non-smoothness that the Coulomb model introduces about zero sliding velocity can be reduced by many different ways, such as velocity regularization of the stiction force. Here, this is achieved using a *bristle approach*, which defines a stiffness k_T in the tangential directions, so that the stiction force is

$$\boldsymbol{\lambda}_T = -k_T \mathbf{s} \tag{9}$$

where $\mathbf{s}$ contains the two components of the *average bristle deflection* (or *deflection*), which represents the elastic deformation of the contact interface.

The deflection cannot be computed using the configuration of the system, because such a quantity depends on "the path" that the system has followed. Therefore, the sliding velocity $\mathbf{v}_T$ needs to be integrated, so that the deflection can be expressed in terms of the generalized velocities as

$$\mathbf{s}^+ = \mathbf{s} + h\mathbf{v}_T^+ = \mathbf{s} + h\mathbf{D}\mathbf{v}^+ \tag{10}$$

The friction force can also be expressed in terms of the generalized velocities,

$$\boldsymbol{\lambda}_T^+ = -k_T \mathbf{s}^+ = -k_T \mathbf{s} - hk_T \mathbf{D}\mathbf{v}^+ = \boldsymbol{\lambda}_T - hk_T \mathbf{D}\mathbf{v}^+ \tag{11}$$

where $\boldsymbol{\lambda}_T = -k_T \mathbf{s}$ is the friction force of the previous time-step. Equation (11) shows how the bristle deflection is not necessary to define the friction force, because all the needed information

regarding the path followed by the system is contained in the friction force.

However, this condition can only be applied in case that the friction force does not exceed the maximum stiction force. Therefore, lower and upper bounds $\underline{\boldsymbol{\lambda}}_T$ and $\overline{\boldsymbol{\lambda}}_T$ are defined for the components of the friction force $\boldsymbol{\lambda}_T^+$ as following

$$\begin{bmatrix} -\mu\lambda_N \\ -\mu\lambda_N \end{bmatrix} = \underline{\boldsymbol{\lambda}}_T \leq \boldsymbol{\lambda}_T^+ \leq \overline{\boldsymbol{\lambda}}_T = \begin{bmatrix} +\mu\lambda_N \\ +\mu\lambda_N \end{bmatrix} \tag{12}$$

where μ is the friction coefficient, and λ_N is the normal contact force resulting from the previous time-step. Nevertheless, a few iterations can be performed in order to make the boundaries tend to $\pm\mu\lambda_N^+$ [10].

Additionally, in order to improve the accuracy of the stick-slip transition, the basis defined in the tangent plane can be modified, so that the previous friction force $\boldsymbol{\lambda}_T$ is aligned with one direction

$$\boldsymbol{\lambda}_T = \begin{bmatrix} -\lambda_{T1} \\ 0 \end{bmatrix} \tag{13}$$

Then, the generalized friction force can be expressed as follows

$$\mathbf{f}_{\text{fric}} = \mathbf{D}^{\text{T}} \boldsymbol{\lambda}_T = \mathbf{D}^{\text{T}} \mathbf{R} \hat{\boldsymbol{\lambda}}_T = \hat{\mathbf{D}}^{\text{T}} \hat{\boldsymbol{\lambda}}_T \tag{14}$$

where $\hat{\boldsymbol{\lambda}}_T = \mathbf{R}^{\text{T}} \boldsymbol{\lambda}_T$ contains the components of the friction force using any other basis, and $\mathbf{R}$ is the 2×2 orthogonal change of basis matrix.

This procedure changes the boundary enforcement, so that the boundaries in Eqn. (12) are applied to $\boldsymbol{\lambda}_T$, instead of any other arbitrary $\hat{\boldsymbol{\lambda}}_T$. Figure 1 shows the tangent plane with the friction force and the two possible boundaries for it, so it can be seen that the closest slick-slip transition to the force $\boldsymbol{\lambda}_T$ is

$$\boldsymbol{\lambda}_T = \begin{bmatrix} -\mu\lambda_N \\ 0 \end{bmatrix} \tag{15}$$

Kinetic Friction Model

The *kinetic friction model* uses the direction of the sliding velocity (or *sliding direction*) to define the basis in the tangent plane, so that the sliding velocity resulting from the previous time-step has only one non-zero component:

$$\mathbf{v}_T = \mathbf{D}\mathbf{v} = \begin{bmatrix} v_{T1} \\ 0 \end{bmatrix} \tag{16}$$

As seen above, this representation of the sliding velocity can always be achieved by means of a change of basis, so that

$$\mathbf{v}_T = \mathbf{R}\hat{\mathbf{v}}_T = \mathbf{R}\hat{\mathbf{D}}\mathbf{v} = \mathbf{D}\mathbf{v} \tag{17}$$

3
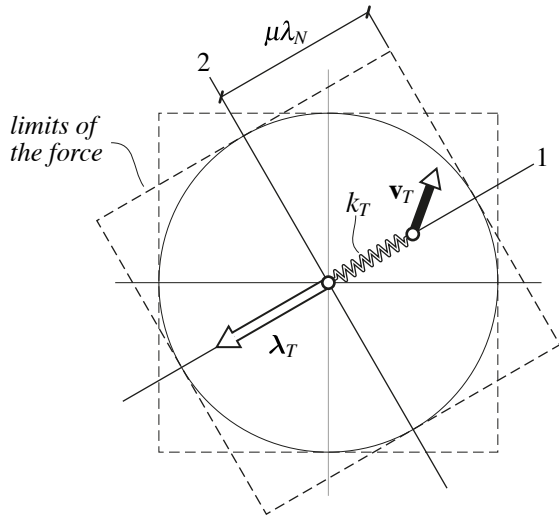
Copyright © 2016 by ASME

FIGURE 1. STATIC FRICTION FORCE WITH LIMITS.

where $\hat{\mathbf{v}}_T = \mathbf{R}^T \mathbf{v}_T$ contains the components of the sliding velocity using any other orthogonal basis in the plane, and $\mathbf{R}$ is the 2×2 change of basis matrix.

The same boundaries in Eqn. (12) are used for the two components of the friction force $\boldsymbol{\lambda}_T$. The component of the friction force along the sliding direction is computed similarly to Eqn. (11)

$$\lambda_{T1}^+ = -\mu \lambda_N - h k_T v_{T1}^+ \tag{18}$$

which will only take values different from $\lambda_{T1} = -\mu \lambda_N$ in case of sliding reversion, i.e., $v_{T1}^+ < 0$.

On the other hand, the component of the friction force along the transversal direction is regularized using the sliding velocity as following

$$\lambda_{T2}^+ = -b_\mu v_{T2}^+ \tag{19}$$

where v_{T2}^+ is the sliding velocity component along the transversal direction, and

$$b_\mu = \frac{\mu \lambda_N}{v_{T1}} \tag{20}$$

is the *drift viscous coefficient* which is updated every time-step.

This regularized model with a hybrid approach between dry and viscous friction aims to reduce the misalignment between the friction force $\boldsymbol{\lambda}_T^+$ and the sliding velocity $\mathbf{v}_T^+$, which happens at some degree in all LCP based formulations [3, 8, 10].
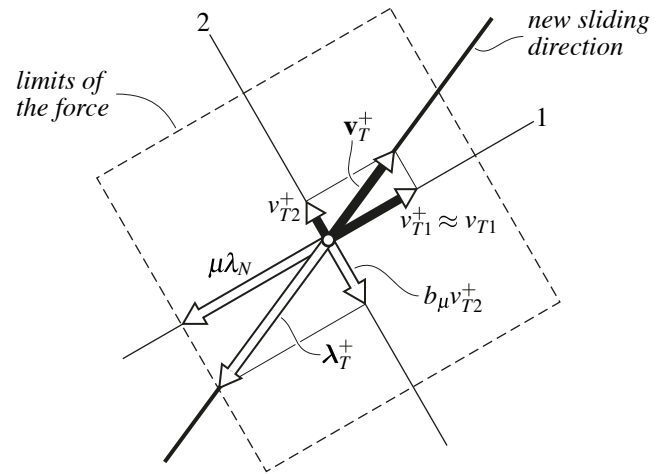

FIGURE 2. KINETIC FRICTION MODEL.

Basically, any deviation of the sliding velocity produced by the component in the transversal direction v_{T2}^+ is compensated by the regularitzation in Eqn. (19), so that there is not misalignment if the velocity component in the sliding direction remains constant, see Fig. 2.

LCP FORMULATION

The main variables of the LCP are the generalized velocities $\mathbf{v}^+$, together with the constraint and friction forces $\boldsymbol{\lambda}^+$, $\boldsymbol{\lambda}_N^+$ and $\boldsymbol{\lambda}_T^+$. Therefore, Eqn. (6) can be expressed in terms of these variables as follows

$$\mathbf{M}\mathbf{v}^+ - \mathbf{A}^T h \boldsymbol{\lambda}^+ - \mathbf{N}^T h \boldsymbol{\lambda}_N^+ - \mathbf{D}^T h \boldsymbol{\lambda}_T^+ = h\mathbf{f}_0 \tag{21}$$

where $\mathbf{f}_0 = \mathbf{f}_{app} - \mathbf{c} + \mathbf{M}\mathbf{v}h^{-1}$ is known. As already mentioned above, all the elements without the $^+$ superscript are computed using the known mechanical state ($\mathbf{q}$ and $\mathbf{v}$) of the system.

Regarding the constraints, and according to Eqn. (2), the generalized velocities $\mathbf{v}^+$ have to satisfy

$$\mathbf{u} = \mathbf{A}\mathbf{v}^+ \tag{22}$$

where $\mathbf{u}(\mathbf{q},t)$ is known. For the unilateral constraints, the normal separation velocity is defined using Eqn. (3) as

$$\dot{\boldsymbol{\Phi}}^+ = \mathbf{N}\mathbf{v}^+ \geq \mathbf{0} \tag{23}$$

Due to its unilateral nature, normal forces $\boldsymbol{\lambda}_N$ cannot be negative, and have to be zero when separation occurs. Therefore, the

following complementarity condition is defined

$$\Phi_i^+ \begin{cases} = 0 & \text{if } \lambda_{Ni}^+ > 0 \\ \geq 0 & \text{if } \lambda_{Ni}^+ = 0 \end{cases} \qquad \forall i = 1 \dots r \qquad (24)$$

The static and kinetic friction models described in Eqns. (11), (18) and (19) can be unified as following

$$\mathbf{D}\mathbf{v}^+ + \tilde{\mathbf{C}}_T h \boldsymbol{\lambda}_T^+ - \tilde{\mathbf{C}}_T h \tilde{\boldsymbol{\lambda}}_T = \boldsymbol{\sigma}^+ \qquad (25)$$

where $\tilde{\mathbf{C}}_T = \text{diag}\left(\tilde{\mathbf{C}}_{T1} \cdots \tilde{\mathbf{C}}_{Tr}\right)$ is a $2r \times 2r$ diagonal matrix and $\tilde{\boldsymbol{\lambda}}_T = \left[\tilde{\boldsymbol{\lambda}}_{T1}^{\mathrm{T}} \cdots \tilde{\boldsymbol{\lambda}}_{Tr}^{\mathrm{T}} \right]^{\mathrm{T}}$ is a $2r \times 1$ array, which depend on the model used, so for the static friction model,

$$\tilde{\mathbf{C}}_{Ti} = \begin{bmatrix} k_{Ti}^{-1} & \\ & k_{Ti}^{-1} \end{bmatrix} h^{-2} \quad \text{and} \quad \tilde{\boldsymbol{\lambda}}_{Ti} = \boldsymbol{\lambda}_{Ti} \qquad (26)$$

and for the kinetic friction model,

$$\tilde{\mathbf{C}}_{Ti} = \begin{bmatrix} k_{Ti}^{-1} & \\ & hb_{\mu i}^{-1} \end{bmatrix} h^{-2} \quad \text{and} \quad \tilde{\boldsymbol{\lambda}}_{Ti} = \begin{bmatrix} -\mu_i \lambda_{Ni} \\ 0 \end{bmatrix} \qquad (27)$$

and $\boldsymbol{\sigma}^+ = \left[\boldsymbol{\sigma}_1^{\mathrm{T}} \cdots \boldsymbol{\sigma}_r^{\mathrm{T}} \right]^{\mathrm{T}}$ is the $2r \times 1$ array of *slack variables* associated with the friction force $\boldsymbol{\lambda}_T^+$, which are defined with the following complementarity condition

$$\sigma_{ij}^+ \begin{cases} \leq 0 & \text{if } \lambda_{Tij}^+ = +\mu_i \lambda_{Ni} \\ \geq 0 & \text{if } \lambda_{Tij}^+ = -\mu_i \lambda_{Ni} \\ = 0 & \text{otherwise} \end{cases} \qquad \begin{matrix} \forall i = 1 \dots r \\ \forall j = 1,2 \end{matrix} \qquad (28)$$

In order to avoid bad numerical behaviour, a small velocity threshold v_{th} is considered to distinguish between sticking and sliding contact points, so that if the value of the sliding velocity is under or equal to it, the static model is applied.

Moreover, this formulation can handle an infinite tangential stiffness, i.e., $k_T \to \infty$, which can give a better approximation of the Coulomb model. In such a case,

$$\tilde{\mathbf{C}}_{Ti} = \mathbf{0} \quad \text{and} \quad \tilde{\mathbf{C}}_{Ti} = \begin{bmatrix} 0 & \\ & h^{-1}b_{\mu i}^{-1} \end{bmatrix} \qquad (29)$$

for the static and kinetic friction models, respectively.

Finally, Equations (21), (22), (23) and (25) can be expressed in the following matrix form

$$\begin{bmatrix} \mathbf{M} & -\mathbf{A}^{\mathrm{T}} & -\mathbf{N}^{\mathrm{T}} & -\mathbf{D}^{\mathrm{T}} \\ \mathbf{A} & \mathbf{0} & \mathbf{0} & \mathbf{0} \\ \mathbf{N} & \mathbf{0} & \mathbf{0} & \mathbf{0} \\ \mathbf{D} & \mathbf{0} & \mathbf{0} & \tilde{\mathbf{C}}_T \end{bmatrix} \begin{bmatrix} \mathbf{v}^+ \\ h\boldsymbol{\lambda}^+ \\ h\boldsymbol{\lambda}_N^+ \\ h\boldsymbol{\lambda}_T^+ \end{bmatrix} + \begin{bmatrix} -h\mathbf{f}_0 \\ -\mathbf{u} \\ \mathbf{0} \\ -\tilde{\mathbf{C}}_T h\tilde{\boldsymbol{\lambda}}_T \end{bmatrix} = \begin{bmatrix} \mathbf{0} \\ \mathbf{0} \\ \dot{\boldsymbol{\Phi}}^+ \\ \boldsymbol{\sigma}^+ \end{bmatrix} \qquad (30)$$

which is known as *Mixed Linear Complementarity Problem with Bounds*. This is the general formulation of a LCP; where some variables have upper and lower bounds, and others are partially or totally unbounded. As mentioned above, the bounds for the main variables are

$$\boldsymbol{\lambda}_N^+ \geq \mathbf{0} \qquad \text{and} \qquad \underline{\boldsymbol{\lambda}}_T \leq \boldsymbol{\lambda}_T^+ \leq \overline{\boldsymbol{\lambda}}_T \qquad (31)$$

with the corresponding slack variables $\dot{\boldsymbol{\Phi}}^+$ and $\boldsymbol{\sigma}^+$. To solve it, the pivoting algorithm proposed by Júdice and Pires [11] can be used.

Regularizing the static friction force using a bristle approach allows the system to cope with redundancy coming from the friction interfaces. As it can be seen in Eqn. (30), the lead matrix can be full rank regardless of the rank of the friction force Jacobian matrix $\mathbf{D}$. Although velocity regularization of the stiction force can solve the same problem, the sliding artifact does not appear when the bristle model is used.

EXAMPLE

In order to assess the accuracy of this model, several simulations have been carried out. In this section, the results of a representative example are shown and compared to other LCP-based formulations: the polygonal approximation of the friction cone [2,3,8] using the formulation proposed by Anitescu and Potra [3], and the box friction model proposed by Lacoursiere [10]. The ideal Coulomb friction model has also been used, so that it can serve as a reference.

A certain initial conditions have been given to the 3D model of a wheel with one single contact point with the ground, so that it slides for the first two seconds, see Fig. 3 and Tab. 1. The objective is to show how the kinetic friction force modelling affects the system behaviour, which is one of the main features of the model presented here. In all the simulations, a time-step frequency of 1kHz is used, except for the ideal Coulomb model where it is 10kHz.

Figure 4 shows the normalized value of the friction force, i.e., its value with respect to $\mu\lambda_N$. As it can be seen, the regularized model gives a better approximation of the Coulomb model compared to the other models, especially during the sliding phase, where it keeps the value close to $\mu\lambda_N$. The normalized
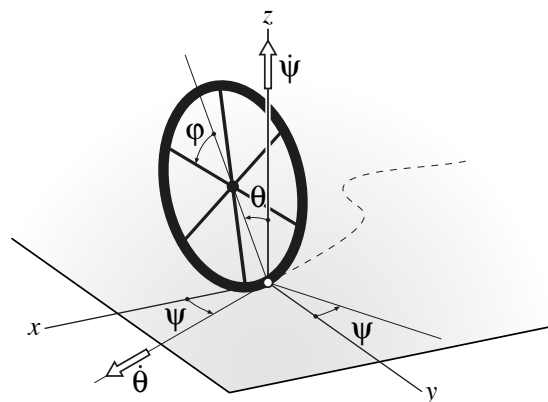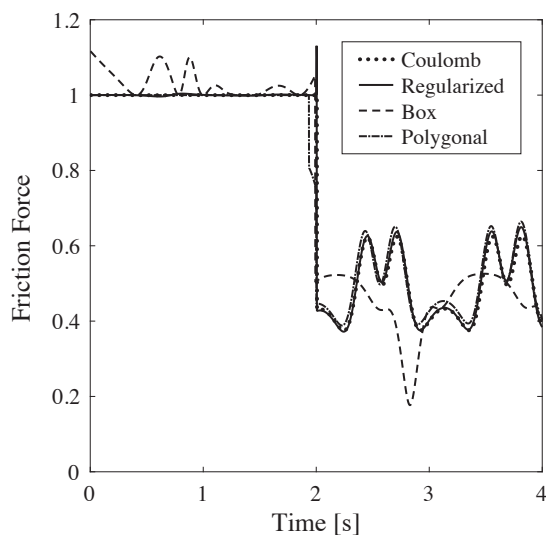
FIGURE 3.   3D MODEL OF A WHEEL.

FIGURE 4.   NORMALIZED VALUE OF THE FRICTION FORCE.

TABLE 1.   SYSTEM PARAMETERS

Wheel		
Radius	R	0.5 m
Mass	m	1 kg
Axial moment of inertia	I_a	0.6 kg m^2
Transversal moments of inertia	I_t	0.3 kg m^2
Contact Model		
Friction coefficient	μ	0.3
Tangential stiffness	k_T	10^{10} N m^{-1}
Sliding velocity threshold	v_{th}	0.01 m s^{-1}
Initial Condition		
Contact distance (*gap function*)	Φ	0 m
Orientation with *Euler angles**		
1st (vertical axis)	ψ	0°
2nd (horizontal diameter)	θ	20°
3rd (wheel axis)	ϕ	0°
Velocity of the COM	$\dot{x}$	6 m s^{-1}
Angular velocity	$\dot{\psi}$	-2 rad s^{-1}
Other generalized velocities		0

*The wheel axis is parallel to the y axis for $\psi = \theta = \phi = 0°$.

root-mean-square deviation with respect to the Coulomb model is 1.67% for the regularized model, compared with 3.76% for the polygonal model, and 9.70% for the box model.

Figure 5.a shows the relative error in the position of the centre of the wheel, normalized using the distance from the starting point, and Fig. 5.b shows the error in the mechanical energy. As it can be seen, both errors are significantly reduced when using the proposed regularized model.

Moreover, the misalignment between the friction force and the sliding velocity, which is shown in Fig. 5.c, is also reduced. The root-mean-square deviation for the regularized model is 0.7°, while for the polygonal and box models are 14.0° and 12.6°, respectively.

In addition, these results suggest that the position is mainly affected by the force misalignment, which is present in the two other models. Even though the polygonal model presents a better approximation of the force value compared to the box model, both have roughly the same position error (see Fig. 5.a).

However, the energy of the system seems to be also sensitive to the fluctuations of the force value. The polygonal model shows less energy error than the box model, whereas the misalignment is similar in both models.

CONCLUSIONS

LCP-based formulations have already proved to be suitable for the efficient simulation of multibody systems with large number of bodies and contacts. The addition of this new friction model improves substantially the simulation accuracy.

The regularization of the kinetic friction force has shown a better approximation of the Coulomb friction model compared to other LCP-based formulations. Namely, the error in the friction force value and its misalignment with respect to the sliding velocity have been considerably reduced.

The regularization of the static friction force using a bristle approach has been incorporated in a LCP formulation, resulting
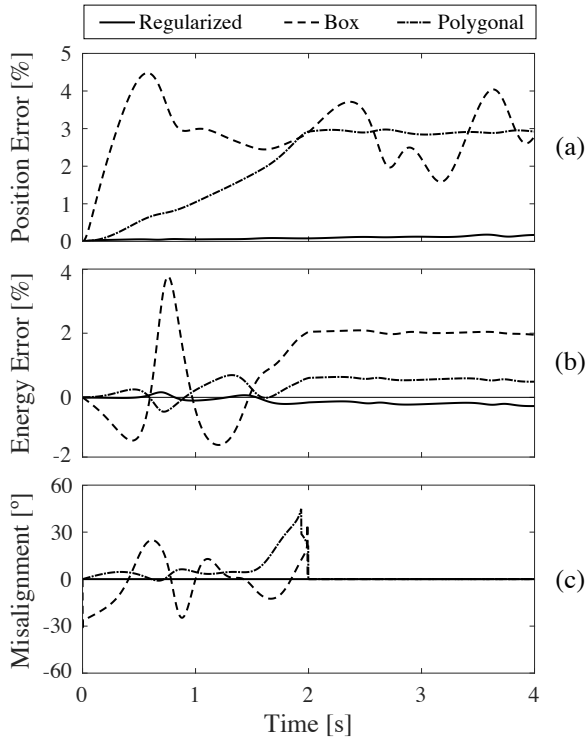
FIGURE 5. POSITION, ENERGY AND MISALIGNMENT ERRORS, COMPARED TO THE COULOMB MODEL.

in a Mixed LCP with bounds. Considering compliance in the tangential directions can handle redundancy coming from the friction interfaces. Although velocity regularization of the stiction force can solve the same problem, the sliding artifact does not appear when the bristle model is used.

It is worth noting that, as far as the authors know, the bristle model has never been included in LCP formulations for multibody systems. These so-called dynamic friction models are usually very detailed and their implementation in large-scale multibody systems can result in a decrease in simulation performance. They also include additional state variables (e.g., the bristle deflection), the evolution of which is governed by additional differential equations.

However, the formulation presented here overcomes this; it exhibits the advantages of the bristle model, such as the position-level regularization with a continuous transition of the static friction force; while, without the addition of other variables, its simulation performance is similar to the other LCP-based formulations.

REFERENCES

[1] Baraff, D., 1989. "Analytical methods for dynamic simulation of non-penetrating rigid bodies". *In Computer Graphics (SIGGRAPH '89 Proceedings),* **23**(3), pp. 223–232.

[2] Glocker, C., 2001. *Set-Valued Force Laws*. Springer, Troy, New York, USA.

[3] Anitescu, M., and Potra, F. A., 1997. "Formulating dynamic multi-rigid-body contact problems with friction as solvable linear complementarity problems". *Nonlinear Dynamics,* **14**, pp. 231–247.

[4] Anitescu, M., Tasora, A., and Stewart, D., 1999. "Time-stepping for three-dimensional rigid body dynamics". *Computer Methods in Applied Mechanics and Engineering,* **177**, pp. 183–197.

[5] Trinkle, J., Pang, J., Sudarsky, S., and Lo, G., 1997. "On dynamic multi-rigid-body contact problems with coulomb friction". *Zeitschrift für Angewandte Mathematik und Mechanik,* **77**, pp. 267–279.

[6] Sauer, J., and Schömer, E., 1998. "A constraint-based approach to rigid body dynamics for virtual reality applications". *Proceedings of the ACM symposium on Virtual reality software and technology*, pp. 153–162.

[7] Son, W., Trinkle, J., and Amato, N., 2001. "Hybrid dynamic simulation of rigid-body contact with coulomb friction". *In Proceedings, IEEE International Conference on Robots and Automation*, pp. 1376–1381.

[8] Stewart, D. E., and Trinkle, J. C., 1996. "An implicit time-stepping scheme for rigid body dynamics with inelastic collisions and coulomb friction". *International Journal for Numerical Methods in Engineering,* **39**, pp. 2673–2691.

[9] Williams, J., Lu, Y., and Trinkle, J. C., 2014. "A complementarity based contact model for geometrically accurate treatment of polytopes in simulation". *ASME 2014 International Design Engineering Technical Conferences and Computers and Information in Engineering Conference,* **6**, p. V006T10A023.

[10] Lacoursière, C., 2006. A regularized time stepper for multibody systems. Tech. Rep. 04, UMINF.

[11] Júdice, J., and Pires, F., 1992. "Basic-set algorithm for a generalized linear complementarity problem". *Journal of optimization theory and applications,* **74**(3), pp. 391–411.

[12] Gonthier, Y., McPhee, J., Lange, C., and Piedboeuf, J. C., 2004. "A regularized contact model with asymmetric damping and dwell-time dependent friction". *Multibody System Dynamics,* **11**(3), pp. 209–233.

[13] Liang, J., Fillmore, S., and Ma, O., 2012. "An extended bristle friction force model with experimental validation". *Mechanism and Machine Theory,* **56**, pp. 123–137.

[14] Haessig, D. A., and Friedland, B., 1991. "On the modeling and simulation of friction". *Journal of Dynamic Systems, Measurement, and Control,* **113**(3), pp. 354–362.

[15] Wit, C. C. D., Olsson, H., Astrom, K. J., and Lischinsky, P., 1995. "A new model for control of systems with friction". *IEEE Transactions on Automatic Control,* **40**(3), pp. 419–425.